Mathematical Biosciences 368 (2024) 109130

Contents lists available at ScienceDirect

Mathematical Biosciences

journal homepage: www.elsevier.com/locate/mbs

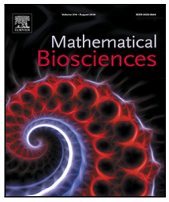

Original Research Article

Population dynamics of a stoichiometric aquatic tri-trophic level model with fear effect☆

Pingping Cong [a,b], Meng Fan [a,*], Xingfu Zou [c]

[a] School of Mathematics and Statistics, National Center for Applied Mathematics in Jilin, Center for Mathematical Biosciences, Northeast Normal University, Changchun, Jilin, 130024, China
[b] School of Biomedical Engineering, Guangdong Medical University, Dongguan, Guangdong, 523808, China
[c] Department of Applied Mathematics, University of Western Ontario, London, ON, N6A 5B7, Canada

ARTICLE INFO

Keywords:
Stoichiometry
Fear effect
Aquatic ecosystem
Light and phosphorus
Chaotic dynamics

ABSTRACT

In this paper, a stoichiometric aquatic tri-trophic level model is proposed and analyzed, which incorporates the effect of light and phosphorus, as well as the fear effect in predator–prey interactions. The analysis of the model includes the dissipativity and the existence and stability of equilibria. The influence of environmental factors and fear effect on the dynamics of the system is particularly investigated. The key findings reveal that the coexistence of populations is positively influenced by an appropriate level of light intensity and/or the dissolved phosphorus input concentration; however, excessive levels of phosphorus input can disrupt the system, leading to chaotic behaviors. Furthermore, it is found that the fear effect can stabilize the system and promote the chances of population coexistence.

1. Introduction

The composition and balance of some key chemical elements within an ecosystem are closely tied to the energy flow in a food web and vital ecological functions [1,2]. Ecological stoichiometry can be simply defined as the biology of elements from molecules to the biosphere [3], and can provide a valuable framework for analyzing the impact of the elemental composition of organisms and their food on production, nutrient cycling, and food web dynamics [3–5]. As an emerging field of research, the theory of ecological stoichiometry has a significant role to play in understanding and managing ecosystems.

Phytoplankton, as the primary producers in aquatic ecosystems, are reliant on two critical resources for their growth and reproduction: light and nutrient [6]. Through photosynthesis, phytoplankton convert the resources into organic carbon, while also absorbing phosphorus from the surrounding water. Carbon is the fundamental building block of phytoplankton and is used to measure the biomass of a population. Phosphorus is the limiting element for population growth, and the ratio of phosphorus to carbon in phytoplankton directly determines the quality of phytoplankton as food for upper level species [7]. A low ratio indicates inferior phytoplankton quality, while a high ratio implies superior quality. Ecological stoichiometry provides a powerful method for characterizing the changes in phytoplankton quality and has been utilized in mathematical modeling to study aquatic ecosystems [2,8–18].

Loladze et al. [2] developed the well-known LKE model, which applies stoichiometric principles to a producer-grazer system, and demonstrated the critical impact of energy and nutrient enrichment on the system. Wang et al. [8] modeled the ecological stoichiometry of bacteria-algae interactions in the epilimnion and explored the effects of varying light and phosphorus availability on the system. To account for the multiple impacts of phytoplankton stoichiometry on higher trophic levels and their feedback, Peace [17] formulated a three-dimensional model and demonstrated the interplay of nutrients, light, and food chain length in determining the ecological transfer efficiency. Chen et al. [14] proposed a stoichiometric food chain model with two limiting nutrients, which demonstrates that stoichiometry can narrow the parameter space of chaotic dynamics. They also observed that while the decrease in producer production efficiency may have minimal effects on the growth of consumers, it can significantly impact top predators' growth. Therefore, the models incorporating stoichiometry can play a crucial role in shaping the structure and diversity of aquatic food webs.

☆ Pingping Cong is funded by the National Natural Science Foundation of China (No. 12071068) and the China Scholarship Council (No. 202106620028); Meng Fan is funded by the National Natural Science Foundation of China (No. 12071068); Xingfu Zou is funded by the Natural Sciences and Engineering Research Council of Canada (No. RGPIN-2022-04744).

* Corresponding author.
E-mail address: mfan@nenu.edu.cn (M. Fan).

https://doi.org/10.1016/j.mbs.2023.109130
Received 18 August 2023; Received in revised form 4 December 2023; Accepted 12 December 2023
Available online 14 December 2023

Within an aquatic ecosystem, a common and typical food web is composed of phytoplankton, zooplankton, and fish. The phytoplankton is preyed upon by zooplankton, and in turn, the zooplankton is consumed by some fish. Some fish can feed on both zooplankton and phytoplankton, and this grants a structure of intraguild predation among the three populations. Apart from direct predation between fish and zooplankton, it has been observed that some zooplankton can detect danger from fish by perceiving the scent of predators or alarm substances on their injured counterparts. This detection leads to changes in the predation behavior of the zooplankton, including immobility (dead-men behavior), aggregation, and deliberate cessation of feeding and migration to less food-profitable hypolimnetic habitats, where they are safer [19–21]. Such a change inevitably reduces the zooplankton's predation on the phytoplankton. This strongly suggests/justifies the importance of considering the fear effect in aquatic ecosystems.

We point out that the significance of fear effect of the predator on prey has been demonstrated in experiments with other populations as well. Pangle et al. [22] investigated the fear effect of spiny water flea (Bythotrephes longimanus) on zooplankton and found that an avoidance response of zooplankton to predation emerged. They also discovered that the fear effect on the plankton's growth rate was over seven times greater than the direct predation. Similarly, in a field experiment on the fear effect on song sparrows by their predators, Zanette et al. [23] observed a decline of approximately 40% in the number of offspring of song sparrows throughout the breeding season, which was attributed to the birds' perceiving the risk from its predators. Suraci et al. [24] conducted experiments that showed how the fear effect triggered a trophic cascade that influenced the evolution of system diversification and community structure. All these findings, together with other massive evidence not mentioned here, suggest that the indirect (non-predating or nonlethal) effects between fish and zooplankton in aquatic ecosystems should not be underestimated.

The fear effect has been extensively and intensively explored in recent years by dynamic models. For example, Wang et al. [25] developed a mathematical model that incorporates the reproductive cost of the fear effect; and by analyzing the model, they found that the fear effect could stabilize the predator–prey system. In Wang and Zou [26], the authors used the framework of [25] to model the fear effect for the scenario of the food chain system reported in [24], and theoretically explained the mechanisms of trophic cascade there. In the context of aquatic food chains, [27–29] investigated the impact of the fear effect on the system. However, to the authors' knowledge, there is no modeling work that incorporates both the fear effect and the impact of multiple chemical elements in aquatic systems. This motivates the main goal of this study: incorporating both stoichiometric mechanism and fear effect into a phytoplankton-zooplankton-fish model to enhance our understanding of the population dynamics of such an aquatic ecosystem.

The rest of the paper is organized as follows. Section 2 presents a detailed description of the model formulation process. In Section 3, we conduct a qualitative analysis that includes examining the dissipativity of solutions, as well as exploring the existence and stability of equilibria. The impact of phosphorus input concentration, light intensity, fear effect, and fish's food habits on population density and dynamics of the model is then explored through numerical simulations in Section 4. Finally, in Section 5, we briefly summarize the main results and interpret their biological implications; we also briefly discuss possible future work in the line of this paper.

2. Model formulation

In this section, we formulate a stoichiometric model for an aquatic environment that incorporates inflow and outflow. Specifically, we consider a well-mixed water area with a fixed water depth of L, such as an epilimnion or a shallow lake (see Fig. 1). The model consists of five complex nonlinear ordinary differential equations that capture the rates of change of the biomass of phytoplankton (P), phytoplankton phosphorus cell quota (Q), the concentration of dissolved phosphorus (N), the biomass of zooplankton (Z), and the biomass of fish (F). The growth of phytoplankton is dependent on the intensity of light and the availability of phosphorus. Additionally, we demonstrate how stoichiometry can introduce 'food quality' into the model to influence the production efficiency of the zooplankton and fish. Furthermore, the fear effect between zooplankton and fish is incorporated into this model. All biologically significant variables and parameters in the model and their actual values are listed in Table 1.

Light and phosphorus are essential resources for phytoplankton growth. Note that the light intensity in the water column is absorbed by the water and phytoplankton. Following Lambert–Beer's law [8,43], the light intensity at the water column depth of x can be expressed as

$$I(x,P) = I_0 \exp\left[-(K_{bg} + k_0 P)x\right],\ 0 < x < L,$$

and accordingly, the growth function of phytoplankton $\mu(P,Q)$ is given by

$$\mu(P,Q) = r\left(1 - \frac{Q_{\min}}{Q}\right)\bar{I}(P).$$

Here

$$\bar{I}(P) = \frac{1}{L}\int_0^L \frac{I(x,P)}{I(x,P)+h}dx = \frac{1}{L(K_{bg}+k_0P)}\ln\left(\frac{I_0+h}{I(L,P)+h}\right)$$

and $Q_{\min}$ is the minimum cell quota of phytoplankton at which growth ceases.

By [8,30], the phosphorus uptake rate by phytoplankton is $\rho(Q)g(N)$, where

$$g(N) = \frac{N}{l+N},\quad N \geq 0;$$
$$\rho(Q) = \delta\frac{Q_{\max}-Q}{Q_{\max}-Q_{\min}},\quad Q_{\min} \leq Q \leq Q_{\max}.$$

When the phytoplankton phosphorus cell quota reaches the minimum value $Q_{\min}$, the phosphorus uptake rate becomes a saturating function of N, while there is no uptake when the cell quotas are at their maximum value $Q_{\max}$. Additionally, for phytoplankton, the cell quota dilution rate is proportional to its growth rate [33]. The variation in dissolved phosphorus concentration N is determined by the consumption of phytoplankton $\rho(Q)g(N)P$ and phosphorus exchange $(D/L)(N_0 - N)$ at the water column, where the constant dissolved phosphorus input concentration is denoted by N_0.

Based on the above background preparation, the interactions between the phytoplankton, phytoplankton phosphorus cell quota, dissolved phosphorus concentration, zooplankton, and fish can be described by the following ODE system

$$\begin{aligned}
\frac{dP}{dt} &= rP\left(1 - \frac{Q_{\min}}{Q}\right)\bar{I}(P) - f_1(P)Z - f_2(P)F - d_pP,\\
\frac{dQ}{dt} &= \rho(Q)g(N) - rQ\left(1 - \frac{Q_{\min}}{Q}\right)\bar{I}(P),\\
\frac{dN}{dt} &= \frac{D}{L}(N_0 - N) - \rho(Q)g(N)P,\\
\frac{dZ}{dt} &= e_1f_1(P)Z - q(Z)F - d_zZ,\\
\frac{dF}{dt} &= e_2q(Z)F + e_3f_2(P)F - d_fF.
\end{aligned} \tag{2.1}$$

Here d_p, d_z, and d_f represent the death rates of phytoplankton, zooplankton, and fish, respectively; $f_1(P)$ and $f_2(P)$ represent the uptake rates of phytoplankton by zooplankton and fish, respectively; $q(Z)$ represents the predation rate of fish on zooplankton; e_1, e_2 and e_3 are the maximum nutrient conversion rates of zooplankton and fish, respectively. According to the second law of thermodynamics, $e_i < 1, i = 1,2,3$. The diagram in Fig. 1 visually illustrates the interactions described in (2.1).

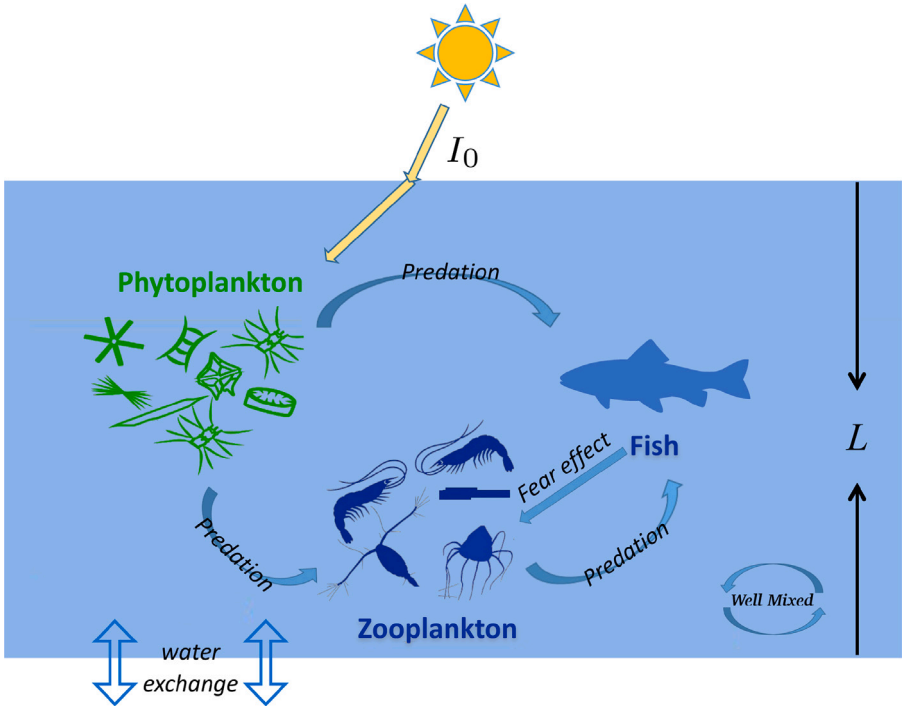

Fig. 1. Phytoplankton-zooplankton-fish interactions in the well-mixed water column. Here I_0 is light intensity at the water surface, and L is the depth of the water column.

Table 1
Variables and parameters of model (2.2) with biological meanings.

Symbol	Meaning	Values	Units	Source
t	Time	Variables	day	
x	Depth	Variables	m	
P	Biomass density of phytoplankton	Variables	mgC/m^3	
Q	Phytoplankton phosphorus cell quota	Variables	mgP/mgC	
N	Concentration of dissolved phosphorus	Variables	mgP/m^3	
Z	Biomass density of zooplankton	Variables	mgC/m^3	
F	Biomass density of fish	Variables	mgC/m^3	
I_0	Light intensity at the water surface	0–800	μmol(photons)/(m^{2}s)	[30,31]
L	Depth of the water column	4.3 (2-10)	m	[32]
k_{bg}	Background light attenuation coefficient	0.5 (0.3-0.9)	m^{-1}	[30,33]
k_0	Light attenuation coefficient of phytoplankton	0.0003	m^2/mgC	[30,33]
h	Light-limited half saturation constant of phytoplankton	200	μmol(photons)/(m^{2}s)	[34]
r	Maximum production rate of phytoplankton	1	day^{-1}	[34,35]
$Q_{\min}$	Minimum phosphorus cell quota of phytoplankton	0.004	mgP/mgC	[30]
$Q_{\max}$	Maximum phosphorus cell quota of phytoplankton	0.04	mgP/mgC	[30]
d_p	Loss rate of phytoplankton	0.1	day^{-1}	[14,35,36]
l	Phosphorus half saturation constant of phytoplankton	1.5	mgP/m^3	[37]
D	Water exchange rate	0.02	m/day	[33]
N_0	Dissolved phosphorus input concentration	0–150	mgP/m^3	[33]
Q_z	Zooplankton phosphorus cell quota	0.03	mgP/mgC	[14,38,39]
Q_f	Fish phosphorus cell quota	0.013	mgP/mgC	[14,40,41]
δ	Maximum phosphorus uptake rate of phytoplankton	0.6 (0.2-1)	mgP/mgC/day	[14,30,33]
e_1	Maximal production efficiency for zooplankton	0.8	–	[14,38,39]
e_2	Maximal production efficiency for fish from zooplankton	0.3	–	Assumption
e_3	Maximal production efficiency for fish from phytoplankton	0.1	–	Assumption
d_z	Loss rate of zooplankton	0.2	day^{-1}	[14,38,39]
d_f	Loss rate of fish	0.003	day^{-1}	[14,40,41]
a_1	Consumption rate of zooplankton	0.81	(mgC/m^3)$^{-1}$ day^{-1}	[14,38,39]
h_1	Time spent by zooplankton for handling phytoplankton	0.3	day	[42]
α	Level of fear effect	>0	(mgC/m^3)$^{-1}$	[42]
β	Search efficiency of the fish population	1	–	[42]
a_2	Rate at which fish attack zooplankton	0.03	day^{-1}	[14,40,41]
a_3	Rate at which fish attack phytoplankton	0.01	day^{-1}	Assumption
γ	Half-saturation constant when fish consume zooplankton	0.75	mgC/m^3	[14,40,41]
γ_2	Half-saturation constant when fish consume phytoplankton	25	mgC/m^3	Assumption

Note that the biological growth is influenced by many factors. In aquatic ecosystems, the phosphorus-to-carbon ratio is used to characterize the quality of phytoplankton. Since both zooplankton and fish consume the phytoplankton, their production/growths are affected not only by the abundance (P) but also by the quality (Q) of the phytoplankton. In other words, quality variable $Q = Q(t)$ may affect the

production efficiency of the zooplankton and fish. In order to incorporate the impact of Q on production efficiency through stoichiometry, we follow [44] to assume that the zooplankton and fish each has an (approximately) constant phosphorous-carbon ratio, denoted by Q_z and Q_f (mgP/mgC) respectively. Then, as in [45], two scenarios are considered:

- if $Q > Q_z$ (resp. $Q > Q_f$), then the phytoplankton is the optimal/best food for the zooplankton (resp. fish). Here, 'optimal' is in the sense that the zooplankton (resp. fish) can maximize the use of energy (carbon) in the food, while in the meantime, 'wastes' the excessive phosphorus (than needed) from what it intakes. The respective production efficiency of zooplankton and fish in this scenario should reach the maximal efficiency e_1 (resp. e_3);
- if $Q < Q_z$ (resp. $Q < Q_f$), then the ingested C contained in P will not be fully utilized and the growth efficiency will be reduced to $e_1 Q/Q_z$ (resp. $e_3 Q/Q_f$).

Combining the above two scenarios, the production efficiencies for zooplankton and fish on consumption of the phytoplankton in (2.1) are then respectively revised to

$$e_1 \min\left\{1, \frac{Q}{Q_z}\right\} \quad \text{and} \quad e_3 \min\left\{1, \frac{Q}{Q_f}\right\}.$$

Likewise, we also follow [14] to introduce a minimum function to reflect the effect of zooplankton quality on the growth efficiency of fish on the zooplankton as follows:

$$e_2 \min\left\{1, \frac{Q_z}{Q_f}\right\}.$$

Note that this is just a new constant replacing e_2, but we will use it to show its dependence on the two threshold values Q_z and Q_f.

Next, we discuss the three functional response functions f_1, f_2, and q. According to [21,46], zooplanktons can sense the risk of predation and respond accordingly by moving to safer places and reducing their own foraging effort. Such a response will lead to a lower predation rate of zooplankton on phytoplankton. In order to incorporate such a reduction of zooplankton's predation rate on phytoplankton due to fear against fish, we use the classical Holling's time budget argument as was done in [42] to obtain the following form for

$$f_1(P, F) = \frac{a_1 P}{1 + a_1 h_1 P + \alpha F},$$

where α denotes the fear level of fish in the zooplankton population. For f_2 and q, we adopt the widely used Holling Type II responses

$$q(Z) = \frac{\beta a_2 Z}{\gamma + Z} \quad \text{and} \quad f_2(P) = \frac{a_3 P}{\gamma_2 + P}.$$

Here, since the anti-predator behavior of zooplankton will reduce its own risk of being predated, we introduce a parameter $\beta \in (0, 1]$ to account for such a benefit.

Combining all above discussions and preparations, the model (2.1) is then modified to

$$\begin{aligned}
\frac{dP}{dt} &= rP\left(1 - \frac{Q_{\min}}{Q}\right)\bar{I}(P) - \frac{a_1 P}{1 + a_1 h_1 P + \alpha F} Z - \frac{a_3 P}{\gamma_2 + P} F - d_p P,\\
\frac{dQ}{dt} &= \rho(Q) g(N) - rQ\left(1 - \frac{Q_{\min}}{Q}\right)\bar{I}(P),\\
\frac{dN}{dt} &= \frac{D}{L}(N_0 - N) - \rho(Q) g(N) P,\\
\frac{dZ}{dt} &= e_1 \min\left\{1, \frac{Q}{Q_z}\right\} \frac{a_1 P}{1 + a_1 h_1 P + \alpha F} Z - \frac{\beta a_2 Z}{\gamma + Z} F - d_z Z,\\
\frac{dF}{dt} &= e_2 \min\left\{1, \frac{Q_z}{Q_f}\right\} \frac{\beta a_2 Z}{\gamma + Z} F + e_3 \min\left\{1, \frac{Q}{Q_f}\right\} \frac{a_3 P}{\gamma_2 + P} F - d_f F,
\end{aligned} \tag{2.2}$$

which is the working model for this paper. Due to the biological background and significance, we study the solutions of the model with initial values satisfying

$$P(0) > 0, N(0) > 0, Z(0) > 0, F(0) > 0, Q_{\min} \le Q(0) \le Q_{\max}. \tag{2.3}$$

3. Model analyses

3.1. Preliminaries

In this section, we investigate the dynamics of system (2.2). First, the nonlinear term in system (2.2) satisfies local Lipschitz continuity, thus there exists a T_0 such that the solution of system (2.2) exists locally and is unique for $t \in (0, T_0)$.

Let $S(t) = (P(t), Q(t), N(t), Z(t), F(t))$ be a solution of (2.2), assume that there exists a time $t_1 > 0$ such that $Q(t_1) = Q_{\min}$ for the first time, so

$$\left.\frac{dQ}{dt}\right|_{t_1} > 0,$$

which leads to a contradiction. Similarly, $N(t)$ keeps positive for given positive initial conditions. To facilitate the subsequent analysis, we will express system (2.2) into the following simplified form

$$\frac{dP}{dt} =: PO_1(P, Z, F), \quad \frac{dZ}{dt} =: ZO_2(P, Z, F), \quad \frac{dF}{dt} =: FO_3(P, Z, F).$$

It follows from (2.2) that

$$\begin{aligned}
P(t) &= P(0)\exp\left(\int_0^t O_1(P(s), Z(s), F(s))ds\right),\\
Z(t) &= Z(0)\exp\left(\int_0^t O_2(P(s), Z(s), F(s))ds\right),\\
F(t) &= F(0)\exp\left(\int_0^t O_3(P(s), Z(s), F(s))ds\right),
\end{aligned}$$

which implies that solutions with initial conditions in

$$\Omega := \{(P, Q, N, Z, F) \in \mathbb{R}^5_+ \,\big|\, P, N, Z, F \ge 0, Q_{\min} \le Q \le Q_{\max}\}$$

remain there for all forward times. Then for the system, Ω is the positively invariant set.

Theorem 3.1. *System (2.2) is dissipative, and the set*

$$\overline{\Omega} := \left\{(P, Q, N, Z, F) \in \Omega \,\Big|\, PQ + N + Q_{\min}(Z + F) \le \frac{DN_0}{Ld}\right\}$$

is an invariant and globally attractive region.

Proof. Let $Y = PQ + N + Q_{\min}(Z + F)$, then

$$\begin{aligned}
\frac{dY}{dt} =& \frac{dP}{dt}Q + \frac{dQ}{dt}P + \frac{dN}{dt} + Q_{\min}\frac{d(Z + F)}{dt}\\
=& \mu(P, Q)PQ - d_p PQ - \frac{a_1 PZQ}{1 + a_1 h_1 P + \alpha F} - \frac{a_3 PFQ}{\gamma_2 + P}\\
&+ \rho(Q) g(N) P - \mu(P, Q) QP\\
&+ \frac{D}{L}(N_0 - N) - \rho(Q) g(N) P + e_1 \min\left\{1, \frac{Q}{Q_z}\right\} \frac{a_1 PZQ_{\min}}{1 + a_1 h_1 P + \alpha F}\\
&- d_z Q_{\min} Z\\
&- \frac{\beta a_2 ZFQ_{\min}}{\gamma + Z} + e_2 \min\left\{1, \frac{Q_z}{Q_f}\right\} \frac{\beta a_2 ZFQ_{\min}}{\gamma + Z}\\
&+ e_3 \min\left\{1, \frac{Q}{Q_f}\right\} \frac{a_3 PFQ_{\min}}{\gamma_2 + P} - d_f Q_{\min} F\\
\le& - d_p PQ + \frac{D}{L}(N_0 - N) - d_z Q_{\min} Z - d_f Q_{\min} F\\
\le& \frac{DN_0}{L} - dY,
\end{aligned}$$

where $0 < Q_{\min} \le Q \le Q_{\max}$ and $d = \min\{d_p, d_z, d_f, D/L\}$. Then it implies that

$$\limsup_{t \to \infty} Y(t) \le \frac{DN_0}{Ld}.$$

In conclusion, system (2.2) is dissipative and the set $\overline{\Omega}$ is a globally attracting region. □

According to Theorem 3.1, the solution of this system is bounded, so $T_0 = +\infty$, i.e., the solution of system (2.2) exists uniquely for $(0, +\infty)$.

3.2. Existence and stability of equilibria

System (2.2) has four types of possible boundary equilibria: $E_1 = (0, Q_1, N_0, 0, 0)$, $E_2 = (P_2, Q_2, N_2, 0, 0)$, $E_3 = (P_3, Q_3, N_3, Z_3, 0)$, $E_4 = (P_4, Q_4, N_4, 0, F_4)$, and an internal equilibrium $E^* = (P^*, Q^*, N^*, Z^*, F^*)$.

Theorem 3.2. *The equilibrium $E_1 = (0, Q_1, N_0, 0, 0)$ always exist. If $d_p > R_1$, then E_1 is locally asymptotically stable and is unstable if the inequality does not hold, where*

$$R_1 = r\left(1 - \frac{Q_{\min}}{Q_1}\right)\bar{I}(0), \quad Q_1 = \frac{rQ_{\min}\bar{I}(0)(Q_{\max} - Q_{\min}) + \delta g(N_0)}{r\bar{I}(0)(Q_{\max} - Q_{\min}) + \delta g(N_0)}.$$

Proof. A direct calculation confirms the existence of E_1. At E_1, the Jacobian matrix takes the form

$$J(E_1) = \begin{pmatrix} r\left(1 - \frac{Q_{\min}}{Q_1}\right)\bar{I}(0) - d_p & 0 & 0 & 0 & 0 \\ r(Q_{\min} - Q_1)\bar{I}'(0) & \rho'(Q_1)g(N_0) - r\bar{I}(0) & \rho(Q_1)g'(N_0) & 0 & 0 \\ -\rho(Q_1)g(N_0) & 0 & -\frac{D}{L} & 0 & 0 \\ 0 & 0 & 0 & -d_z & 0 \\ 0 & 0 & 0 & 0 & -d_f \end{pmatrix}.$$

It is not difficult to see that all characteristic roots of $J(E_1)$ have negative real parts if and only if when $d_p > R_1$, proving the conclusion of the theorem. □

Theorem 3.3. *If $d_p < R_1$, then $E_2 = (P_2, Q_2, N_2, 0, 0)$ exists and it is unique.*

Proof. The equilibrium E_2 is found by solving

$$\begin{cases} r\left(1 - \frac{Q_{\min}}{Q}\right)\bar{I}(P) - d_p = 0, \\ \rho(Q)g(N) - r\left(1 - \frac{Q_{\min}}{Q}\right)\bar{I}(P)Q = 0, \\ \frac{D}{L}(N_0 - N) - \rho(Q)g(N)P = 0. \end{cases} \tag{3.4}$$

By a simple calculation, we obtain

$$N_2 = N_0 - \frac{d_p L}{D}P_2 Q_2, \quad P_2 = \frac{l + N_0 - \rho(Q_2)N_0/d_p Q_2}{l/D(d_p Q_2 - \rho(Q_2))} =: \psi(Q_2). \tag{3.5}$$

Substitute (3.5) into Eq. (3.4), we have

$$\chi(Q_2) := r\left(1 - \frac{Q_{\min}}{Q_2}\right)\bar{I}(\psi(Q_2)) - d_p = 0.$$

According to [8], (2.2) exists a unique equilibrium $E_2 = (P_2, Q_2, N_2, 0, 0)$ if and only if when $d_p < R_1$. □

Next, we address the stability of E_2 when it exits.

Theorem 3.4. *Assume $d_p < R_1$ so that E_2 exists. If*

$$d_z > e_1 \min\left\{1, \frac{Q_2}{Q_z}\right\}\frac{a_1 P_2}{1 + a_1 h_1 P_2}, \quad d_f > e_3 \min\left\{1, \frac{Q_2}{Q_f}\right\}\frac{a_3 P_2}{\gamma_2 + P_2},$$
$$b_1 b_2 > b_3 > 0, \tag{3.6}$$

then E_2 is locally asymptotically stable.

Proof. The Jacobian matrix at E_2 can be written as

$$J(E_2) = \begin{pmatrix} a_{11} & a_{12} & 0 & a_{14} & a_{15} \\ a_{21} & a_{22} & a_{23} & 0 & 0 \\ a_{31} & a_{32} & a_{33} & 0 & 0 \\ 0 & 0 & 0 & a_{44} & 0 \\ 0 & 0 & 0 & 0 & a_{55} \end{pmatrix},$$

where

$$a_{11} = r\left(1 - \frac{Q_{\min}}{Q_2}\right)(\bar{I}(P_2) + \bar{I}'(P_2)P_2) - d_p, \quad a_{12} = \frac{rQ_{\min}P_2\bar{I}(P_2)}{Q_2^2},$$
$$a_{14} = -\frac{a_1 P_2}{1 + a_1 h_1 P_2}, \quad a_{15} = -\frac{a_3 P_2}{\gamma_2 + P_2}, \quad a_{21} = r(Q_{\min} - Q_2)\bar{I}'(P_2),$$
$$a_{22} = \rho'(Q_2)g(N_2) - r\bar{I}(P_2), \quad a_{23} = \rho(Q_2)g'(N_2),$$
$$a_{31} = -\rho(Q_2)g(N_2), \quad a_{32} = -\rho'(Q_2)g(N_2)P_2,$$
$$a_{33} = -\frac{D}{L} - \rho(Q_2)g'(N_2)P_2,$$
$$a_{44} = e_1 \min\left\{1, \frac{Q_2}{Q_z}\right\}\frac{a_1 P_2}{1 + a_1 h_1 P_2} - d_z,$$
$$a_{55} = e_3 \min\left\{1, \frac{Q_2}{Q_f}\right\}\frac{a_3 P_2}{\gamma_2 + P_2} - d_f.$$

Therefore, the corresponding characteristic equation is

$$(\lambda - a_{44})(\lambda - a_{55})(\lambda^3 + b_1\lambda^2 + b_2\lambda + b_3) = 0,$$

where

$$b_1 = -(a_{11} + a_{22} + a_{33}) > 0,$$
$$b_2 = a_{11}(a_{22} + a_{33}) - a_{12}a_{21} + a_{22}a_{33} - a_{23}a_{32},$$
$$b_3 = -a_{11}(a_{22}a_{33} + a_{23}a_{32}) + a_{12}(a_{21}a_{33} - a_{23}a_{31}).$$

By Routh–Hurwitz criterion and (3.6), E_2 is locally asymptotically stable. □

Theorem 3.5. *If $d_z < \min\{e_1/h_1, e_1 Q_3/h_1 Q_z\}$, then $E_3 = (P_3, Q_3, N_3, Z_3, 0)$ exists and it is unique.*

Proof. The equilibrium E_3 is given by

$$\begin{cases} r\left(1 - \frac{Q_{\min}}{Q}\right)\bar{I}(P) - \frac{a_1 Z}{1 + a_1 h_1 P} - d_p = 0, \\ \rho(Q)g(N) - r\left(1 - \frac{Q_{\min}}{Q}\right)\bar{I}(P)Q = 0, \\ \frac{D}{L}(N_0 - N) - \rho(Q)g(N)P = 0, \\ e_1 \min\left\{1, \frac{Q}{Q_z}\right\}\frac{a_1 P}{1 + a_1 h_1 P} - d_z = 0. \end{cases} \tag{3.7}$$

We consider the following two cases.

Case 1. $Q > Q_z$. By calculation, we get

$$P_3 = \frac{d_z}{e_1 a_1 - a_1 h_1 d_z},$$
$$Q_3 = \frac{\delta g(N_3)Q_{\max} + r(Q_{\max} - Q_{\min})\bar{I}(P_3)Q_{\min}}{\delta g(N_3) + r(Q_{\max} - Q_{\min})\bar{I}(P_3)} =: \tau(N_3). \tag{3.8}$$

Substitute (3.8) into Eq. (3.7) produces

$$H(N_3) := (\delta + r(Q_{\max} - Q_{\min})\bar{I}(P_3))N_3^2 + \left[\left(\frac{\delta P_3 L}{D} - N_0 - l\right)(r(Q_{\max} - Q_{\min})\bar{I}(P_3)) - \delta N_0\right]N_3 - lN_0(r(Q_{\max} - Q_{\min})\bar{I}(P_3)) = 0.$$

It is trivial to see that $H(N_3) = 0$ always has a positive root. Therefore, it can be concluded that, when $d_z < e_1/h_1$, there exists a unique equilibrium E_3.

Case 2. $Q < Q_z$. From a simple calculation, it follows that

$$P_3 = \frac{d_z Q_z}{e_1 a_1 Q_3 - a_1 h_1 d_z Q_z} =: f(Q_3),$$

then

$$\frac{D}{L}N_3^2+\left(\frac{D(l-N_0)}{L}+\rho(Q_3)f(Q_3)\right)N_3-\frac{lDN_0}{L}=0,$$

and

$$N_3=\frac{\sqrt{B(Q_3)^2L^2+4lD^2N_0}-B(Q_3)L}{2D}=:\nu(Q_3),$$

where $B(Q_3)=\left(\frac{D(l-N_0)}{L}-\rho(Q_3)f(Q_3)\right)$. It calculates that

$$h(Q_3):=\rho(Q_3)g(\nu(Q_3))-r\left(1-\frac{Q_{\min}}{Q_3}\right)\bar{I}(f(Q_3))Q_3=0.$$

Note that $f'(Q),\rho'(Q)<0$, thus $(f(Q)\rho(Q))'<0$, $B'(Q)>0$. Therefore,

$$\frac{d\nu(Q)}{dQ}=\frac{(B(Q)L/\sqrt{B(Q)^2L^2+4lD^2N_0}-1)B'L}{2D}<0,$$

so $g(\nu(Q))'<0$ and $(\rho(Q)g(\nu(Q)))'<0$, then $h(Q)<0$ and $h(Q_{\min})h(Q_{\max})<0$. Then $h(Q_3)=0$ always has a positive root, and it concludes that, when $d_z<e_1Q_3/h_1Q_z$, E_3 exists and is unique. □

Theorem 3.6. *If*

$$d_f>e_2\min\left\{1,\frac{Q_z}{Q_f}\right\}\frac{\beta a_2Z_3}{\gamma+Z_3}+e_3\min\left\{1,\frac{Q_3}{Q_f}\right\}\frac{a_3P_3}{\gamma_2+P_3},$$
$$b_2,b_3>0,\quad b_0b_1b_2>b_2^2+b_0^2b_3, \tag{3.9}$$

then E_3 is locally asymptotically stable.

Proof. At E_3, the Jacobian matrix is given by

$$J(E_3)=\begin{pmatrix}a_{11}&a_{12}&0&a_{14}&a_{15}\\a_{21}&a_{22}&a_{23}&0&0\\a_{31}&a_{32}&a_{33}&0&0\\a_{41}&a_{42}&0&0&a_{45}\\0&0&0&0&a_{55}\end{pmatrix},$$

where

$$a_{11}=r\left(1-\frac{Q_{\min}}{Q_3}\right)(\bar{I}(P_3)+\bar{I}'(P_3)P_3)-\frac{a_1Z_3}{(1+a_1h_1P_3)^2}-d_p,$$
$$a_{12}=\frac{rQ_{\min}P_3\bar{I}(P_3)}{Q_3^2},\quad a_{14}=-\frac{a_1P_3}{1+a_1h_1P_3},$$
$$a_{15}=\frac{\alpha a_1P_3Z_3}{(1+a_1h_1P_3)^2}-\frac{a_3P_3}{\gamma_2+P_3},\quad a_{21}=r(Q_{\min}-Q_3)\bar{I}'(P_3),$$
$$a_{22}=\rho'(Q_3)g(N_3)-r\bar{I}(P_3),\quad a_{23}=\rho(Q_3)g'(N_3),\quad a_{31}=-\rho(Q_3)g(N_3),$$
$$a_{32}=-\rho'(Q_3)g(N_3)P_3,\ a_{33}=-\frac{D}{L}-\rho(Q_3)g'(N_3)P_3,$$
$$a_{41}=e_1\min\left\{1,\frac{Q_3}{Q_z}\right\}\frac{a_1Z_3}{(1+a_1h_1P_3)^2},$$
$$a_{42}=\begin{cases}\dfrac{e_1a_1P_3Z_3}{Q_z(1+a_1h_1P_3)}, & Q_3<Q_z,\\ 0, & Q_3>Q_z,\end{cases}$$
$$a_{45}=-e_1\min\left\{1,\frac{Q_3}{Q_z}\right\}\frac{\alpha a_1P_3Z_3}{(1+a_1h_1P_3)^2}-\frac{\beta a_2Z_3}{\gamma+Z_3},$$
$$a_{55}=e_2\min\left\{1,\frac{Q_z}{Q_f}\right\}\frac{\beta a_2Z_3}{\gamma+Z_3}+e_3\min\left\{1,\frac{Q_3}{Q_f}\right\}\frac{a_3P_3}{\gamma_2+P_3}-d_f.$$

The characteristic equation of $J(E_3)$ is

$$(\lambda-a_{55})(\lambda^4+b_0\lambda^3+b_1\lambda^2+b_2\lambda+b_3)=0,$$

where

$$b_0=-(a_{11}+a_{22}+a_{33})>0,$$
$$b_1=a_{11}(a_{22}+a_{33}-a_{21})-a_{14}a_{41}+a_{22}a_{33}-a_{23}a_{32},$$
$$b_2=a_{11}(a_{23}a_{32}-a_{22}a_{33})+a_{12}(a_{21}a_{33}-a_{23}a_{31})+a_{14}(a_{22}a_{41}+a_{33}a_{41}-a_{21}a_{42}),$$
$$b_3=a_{14}(a_{23}a_{32}a_{41}-a_{23}a_{31}a_{42}-a_{22}a_{33}a_{41}+a_{21}a_{33}a_{42}).$$

By using the Routh–Hurwitz criterion, from (3.9), it follows that $J(E_3)$ has characteristic roots with negative real parts. Therefore, the theorem is proved. □

The equilibrium $E_4=(P_4,Q_4,N_4,0,F_4)$, where P_4,Q_4,N_4, and F_4 are given by

$$\begin{cases}r\left(1-\dfrac{Q_{\min}}{Q}\right)\bar{I}(P)-\dfrac{a_3F}{\gamma_2+P}-d_p=0,\\ \rho(Q)g(N)-r\left(1-\dfrac{Q_{\min}}{Q}\right)\bar{I}(P)Q=0,\\ \dfrac{D}{L}(N_0-N)-\rho(Q)g(N)P=0,\\ e_3\min\left\{1,\dfrac{Q}{Q_f}\right\}\dfrac{a_3P}{\gamma_2+P}-d_f=0.\end{cases}$$

Following a similar proof approach as (3.9), we can derive the subsequent theorem.

Theorem 3.7. *If $d_f<\min\{e_3a_3,e_3a_3Q_4/Q_f\}$, then $E_4=(P_4,Q_4,N_4,0,F_4)$ exists and it is unique.*

Theorem 3.8. *If*

$$d_z>e_1\min\left\{1,\frac{Q_4}{Q_z}\right\}\frac{a_1P_4}{1+a_1h_1P_4+\alpha F_4}-\frac{\beta\gamma a_2F_4}{(\gamma+Z)^2},\quad \bar{b}_2,\bar{b}_3>0,$$
$$\bar{b}_0\bar{b}_1\bar{b}_2>\bar{b}_2^2+\bar{b}_0^2\bar{b}_3, \tag{3.10}$$

then E_4 is locally asymptotically stable.

Proof. At E_4, the Jacobian matrix is given by

$$J(E_4)=\begin{pmatrix}a_{11}&a_{12}&0&a_{14}&a_{15}\\a_{21}&a_{22}&a_{23}&0&0\\a_{31}&a_{32}&a_{33}&0&0\\0&0&0&a_{44}&0\\a_{51}&a_{52}&0&a_{54}&0\end{pmatrix},$$

where

$$a_{11}=r\left(1-\frac{Q_{\min}}{Q_4}\right)(\bar{I}(P_4)+\bar{I}'(P_4)P_4)-\frac{a_3\gamma_2F_4}{(\gamma_2+P_4)^2}-d_p,$$
$$a_{12}=\frac{rQ_{\min}P_4\bar{I}(P_4)}{Q_4^2},\quad a_{14}=-\frac{a_1P_4}{1+a_1h_1P_4+\alpha F_4},$$
$$a_{15}=-\frac{a_3P_4}{\gamma_2+P_4},\quad a_{21}=r(Q_{\min}-Q_4)\bar{I}'(P_4),$$
$$a_{22}=\rho'(Q_4)g(N_4)-r\bar{I}(P_4),\quad a_{23}=\rho(Q_4)g'(N_4),\quad a_{31}=-\rho(Q_4)g(N_4),$$
$$a_{32}=-\rho'(Q_4)g(N_4)P_4,\quad a_{33}=-\frac{D}{L}-\rho(Q_4)g'(N_4)P_4,$$
$$a_{44}=e_1\min\left\{1,\frac{Q_4}{Q_z}\right\}\frac{a_1P_4}{1+a_1h_1P_4+\alpha F_4}-\frac{\beta\gamma a_2F_4}{(\gamma+Z)^2}-d_z,$$
$$a_{51}=e_3\min\left\{1,\frac{Q_4}{Q_f}\right\}\frac{a_3\gamma_2F_4}{(\gamma_2+P_4)^2},$$
$$a_{52}=\begin{cases}\dfrac{e_3a_3P_4F_4}{Q_f(\gamma_2+P_4)}, & Q_4<Q_f,\\ 0, & Q_4>Q_f,\end{cases}\quad a_{54}=e_2\min\left\{1,\frac{Q_z}{Q_f}\right\}\frac{\beta a_2F_4}{\gamma}.$$

The characteristic equation of $J(E_4)$ is

$$(\lambda-a_{44})(\lambda^4+\bar{b}_0\lambda^3+\bar{b}_1\lambda^2+\bar{b}_2\lambda+\bar{b}_3)=0,$$

where

$$\bar{b}_0=-(a_{11}+a_{22}+a_{33})>0,$$
$$\bar{b}_1=a_{33}(a_{11}+a_{22})+a_{11}a_{22}-a_{12}a_{21}-a_{15}a_{51}-a_{23}a_{32},$$
$$\bar{b}_2=a_{15}(a_{22}a_{51}-a_{21}a_{52})+a_{23}(a_{11}a_{32}-a_{12}a_{31})-a_{33}(a_{11}a_{22}+a_{12}a_{21}-a_{15}a_{51}),$$
$$\bar{b}_3=a_{15}(a_{21}a_{33}a_{52}-a_{22}a_{33}a_{52}-a_{23}a_{31}a_{52}+a_{23}a_{32}a_{51}).$$

Table 2
Existence, uniqueness, and stability of boundary equilibria of (2.2).

Equilibria	Existence and uniqueness	Local stability	Biological significance
E_1	Always	$d_p > R_1$	All the three populations go extinct.
E_2	$d_p < R_1$	$d_z > e_1 \min\left\{1, \frac{Q_2}{Q_z}\right\} \frac{a_1 P_2}{1+a_1 h_1 P_2}$, $d_f > e_3 \min\left\{1, \frac{Q_2}{Q_f}\right\} \frac{a_3 P_2}{\gamma_2 + P_2}$, $b_1 b_2 > b_3 > 0$	Only phytoplankton survives.
E_3	$d_z < \min\left\{\frac{e_1}{h_1}, \frac{e_1 Q_3}{h_1 Q_z}\right\}$	$d_f > e_2 \min\left\{1, \frac{Q_z}{Q_f}\right\} \frac{\beta a_2 Z_3}{\gamma + Z_3} + e_3 \min\left\{1, \frac{Q_3}{Q_f}\right\} \frac{a_3 P_3}{\gamma_2 + P_3}$, $b_2, b_3 > 0$, $b_0 b_1 b_2 > b_2^2 + b_0^2 b_3$	Fish is extinct while zooplankton and fish stably coexist.
E_4	$d_f < \min\left\{e_3 a_3, \frac{e_3 a_3 Q_4}{Q_f}\right\}$	$d_z > e_1 \min\left\{1, \frac{Q_4}{Q_z}\right\} \frac{a_1 P_4}{1+a_1 h_1 P_4 + \alpha F_4} - \frac{\beta\gamma a_2 F_4}{(\gamma+Z)^2}$, $\bar{b}_2, \bar{b}_3 > 0$, $\bar{b}_0 \bar{b}_1 \bar{b}_2 > \bar{b}_2^2 + \bar{b}_0^2 \bar{b}_3$	Zooplankton becomes extinct, phytoplankton and fish stably coexist.

According to the Routh–Hurwitz criterion and (3.10), $J(E_4)$ has characteristic roots with negative real parts. Therefore, E_4 is locally asymptotically stable. □

The positive interior equilibrium $E^* = (P^*, Q^*, N^*, Z^*, F^*)$, where P^*, Q^*, N^*, Z^*, and F^* are solved by the following equation

$$\begin{cases} r\left(1 - \frac{Q_{\min}}{Q}\right) \bar{I}(P) - \frac{a_1 Z}{1 + a_1 h_1 P + \alpha F} - \frac{a_3 F}{\gamma_2 + P} - d_p = 0, \\ \rho(Q) g(N) - r\left(1 - \frac{Q_{\min}}{Q}\right) \bar{I}(P) Q = 0, \\ \frac{D}{L}(N_0 - N) - \rho(Q) g(N) P = 0, \\ e_1 \min\left\{1, \frac{Q}{Q_z}\right\} \frac{a_1 P}{1 + a_1 h_1 P + \alpha F} - \frac{\beta a_2 F}{\gamma + Z} - d_z = 0, \\ e_2 \min\left\{1, \frac{Q_z}{Q_f}\right\} \frac{\beta a_2 Z}{\gamma + Z} + e_3 \min\left\{1, \frac{Q}{Q_f}\right\} \frac{a_3 P}{\gamma_2 + P} - d_f = 0. \end{cases} \tag{3.11}$$

As can be seen in (3.11), the existence criterion of E^* is too complicated to be given. However, due to the deterministic nature of the system, we can analyze the system's dynamics by conducting convenient and convincing numerical analyses.

To illustrate the relationship between the existence and local stability of different boundary equilibria, the sufficient criteria for the existence and uniqueness, and local stability of the boundary equilibria are summarized in Table 2.

4. Numerical simulations

In this section, we investigate the effect of four different key factors (i.e., light, phosphorus, fear effect, and fish's food habits) on the population size and the dynamical behavior of system (2.2) through numerical simulations. The parameter values used in the following numerical simulations and their sources are listed in Table 1.

4.1. Effect of light

Light is a major factor in determining the operation and biological composition of aquatic ecosystem and serves a crucial function as it supplies the energy needed for photosynthesis of phytoplankton. In order to explore the effect of different light intensities on system (2.2) and to provide deeper insights into how the system responds to changes of light intensity, the bifurcation diagram of (2.2) with I_0 being the bifurcation parameter is numerically presented as I_0 increases from 0 to 800 μmol(photons)/(m^2s) (see Fig. 2).

From Fig. 2, it observes that all three populations are unable to survive when light intensity is low ($I_0 \in (0, 60)$). There exists a threshold value (I_0=60) for light intensity. If the light intensity increases above the threshold ($I_0 \in (60, 800)$), then all three populations can coexist. As the light intensity continues to increase, the density of phytoplankton continues to increase (Fig. 2(a)). In other words, higher light intensity promotes the growth of phytoplankton. This phenomenon extensively exists in nature [47] since higher light intensity in summer months leads to faster photosynthesis and an increased growth rate of phytoplankton, which often results in phytoplankton blooms. However, the density of zooplankton suddenly increases first, then decreases, and finally remains constant regardless of the variation of light intensity (Fig. 2 (b)). As illustrated in Fig. 2(c), the density of fish consistently decreases after a sudden rise with increasing light intensity. It implies that the increased light intensity may be detrimental to the fish. In summary, both low and high light intensity are unfavorable for the aquatic ecosystem.

4.2. Effect of phosphorus

As a limiting factor for the growth of phytoplankton, the importance of phosphorus should also be explored and documented [8,47,48]. In system (2.2), the input concentration N_0 of the dissolved phosphorus is an important parameter. The trends of phytoplankton, zooplankton, and fish with varying N_0 and the effect of phosphorus on the dynamics of (2.2) are investigated by plotting the bifurcation diagram with N_0 being the bifurcation parameter (see Fig. 3) and also the phase portraits of (2.2) (see Fig. 4(a)–(c)).

Fig. 3 reveals that, when the input concentration of dissolved phosphorus is very low ($N_0 \in (0, 0.4)$), the zooplankton and fish are unable to survive and the density of phytoplankton increases with the increase of N_0. As N_0 increases further ($N_0 \in (0.4, 1)$), the density of phytoplankton decreases, the zooplankton recovers from extinction, and the density of zooplankton increases. When $N_0 \in (1, 6.2)$, (2.2) stabilizes at an internal equilibrium (Fig. 4(a)), where the densities of phytoplankton and fish increase with increasing N_0, while the density of zooplankton decreases but the change is small. If N_0 continues to increase above the critical value N_0=6.2, the internal equilibrium E^* loses its stability and (2.2) undergoes a supercritical Hopf bifurcation leading to the emergence of a limit cycle (see Fig. 4(b)). As N_0 continues to increase and exceeds the threshold N_0=19, the system eventually admits chaotic behavior and the fish goes to extinction (see Fig. 4(c)). In addition, Fig. 5 also shows the time series (P, Z, F) and such irregular oscillating behavior is representative of the chaotic dynamics.

To conclude, only the moderate level of input concentration of dissolved phosphorus is beneficial to the growth of three populations, both too high and too low input concentrations of dissolved phosphorus are detrimental to the coexistence of populations and the stability of the system.

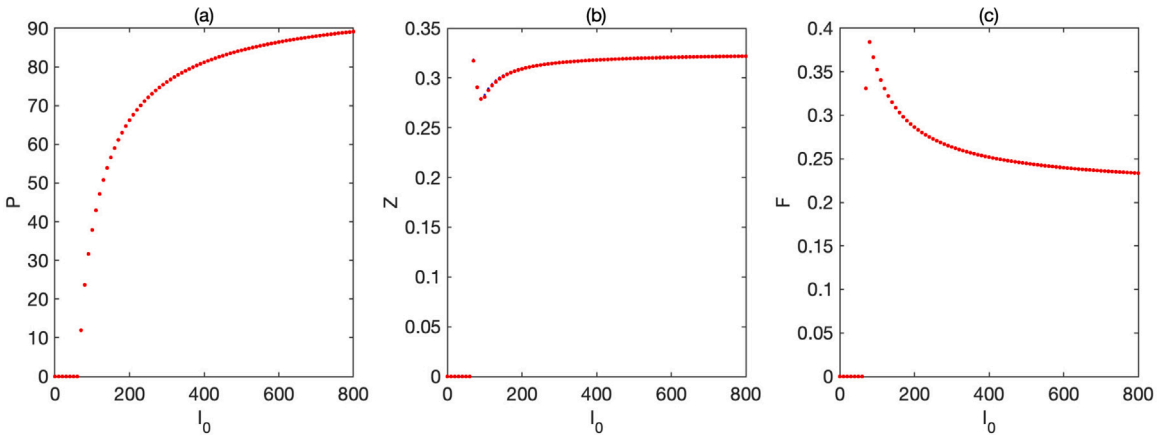

Fig. 2. Effect of light intensity I_0. Here $N_0 = 10, \alpha = 100$, other parameter values are listed in Table 1.

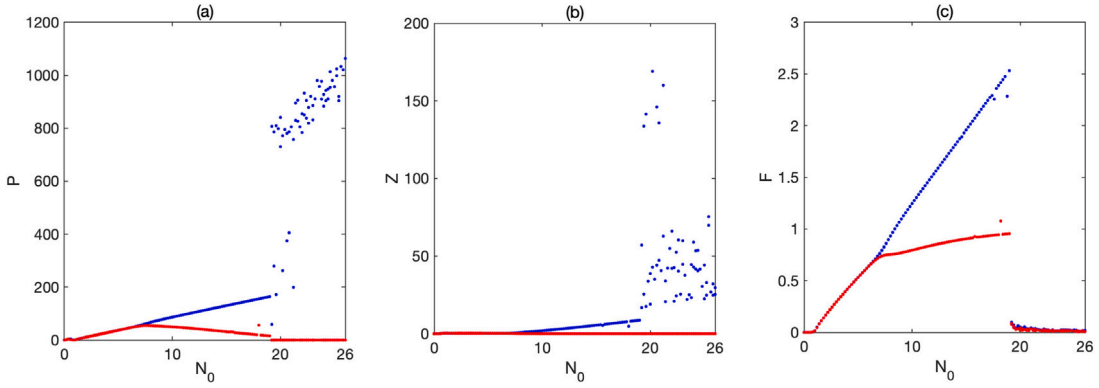

Fig. 3. Effect of the input concentration N_0 of dissolved phosphorus. Here $I_0 = 400, \alpha = 20$, other parameter values are listed in Table 1.

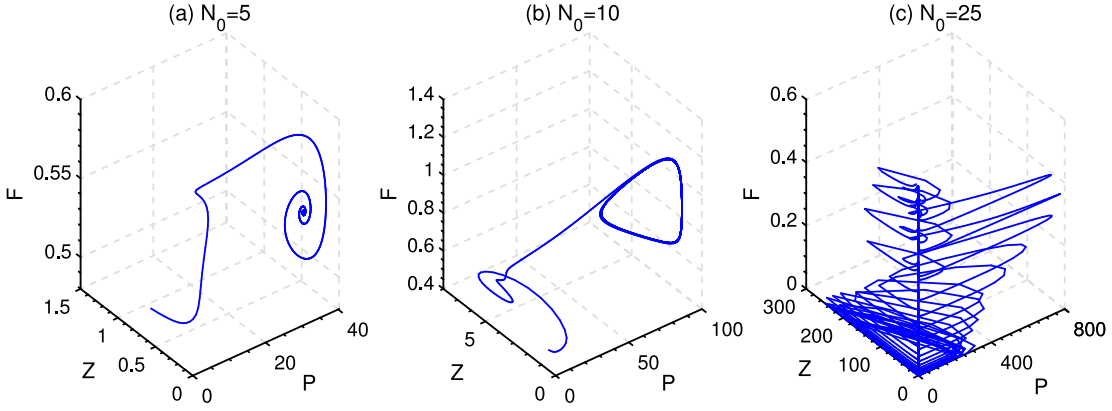

Fig. 4. Attractor of (2.2) in phase space with different N_0. (a) $N_0 = 5$, E^* is an attractor; (b) $N_0 = 10$, the phase trajectories tend to a stable limit circle; (c) $N_0 = 25$, the system exhibits chaotic behavior. Here $I_0 = 400, \alpha = 20$, other parameter values are listed in Table 1, and $P(0) = 0.7$, $Z(0) = 0.6$, and $F(0) = 0.5$.

4.3. Effect of fear

As mentioned above, the fear effect cannot be disregarded and it is essential to consider the effect of fear on dynamics of the aquatic ecosystem. The parameter α in model (2.2) quantifies the intensity of the fear effect. The principal aim of this section is twofold: to investigate how α affects the system's dynamics and to examine its impact on population density. In order to achieve these aims, the bifurcation diagram (Fig. 6) and the maximal Lyapunov exponent diagram (Fig. 7) are presented with α being the target parameter, which characterize the response of the system to the varying fear effect as α increases from 0 to 80.

From Figs. 6 and 7, it follows that, when the fear level α is low ($\alpha \in (0, 15)$), system (2.2) exhibits chaotic dynamics (Fig. 8(a)); as the fear level increases ($\alpha \in (15, 45)$), the system transits from the chaotic regime to the periodic regime (Fig. 8(b)), and the mean values of the cyclic density of phytoplankton tend to rise while the mean values of the cyclic density of zooplankton and fish show the opposite tendency, and the amplitude of the system's cyclic oscillation gradually decreases and eventually diminishes to zero, leading to a stable state through a Hopf bifurcation, as α increases; when α continues to increase and the fear level is large enough ($\alpha \in (45, 80)$), the system undergoes a Hopf bifurcation and converges to a stable internal equilibrium (Fig. 8(c)). In addition, a high level of fear effect is beneficial to phytoplankton

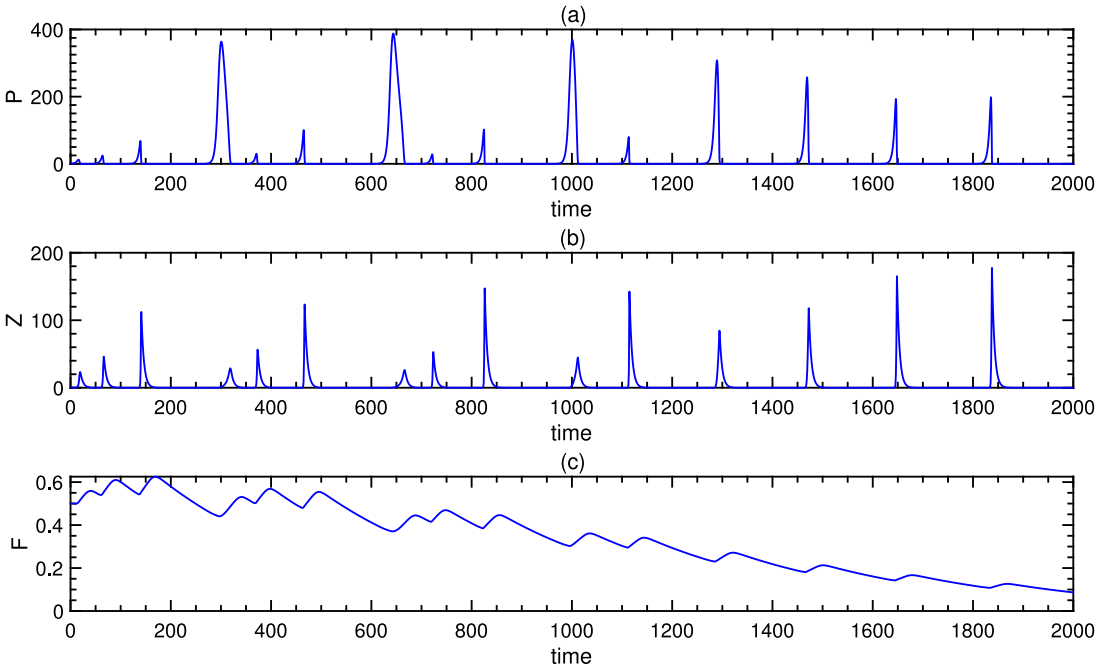

Fig. 5. Time series of (2.2) with $N_0 = 25$. Here $I_0 = 400, \alpha = 20$, other parameter values are listed in Table 1.

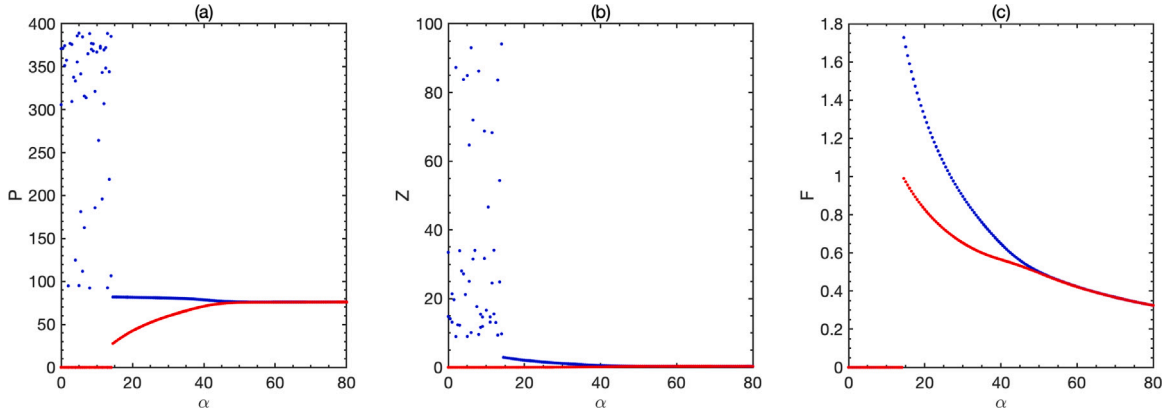

Fig. 6. Effect of the fear factor α. Here $I_0 = 300, N_0 = 10$, other parameter values are listed in Table 1.

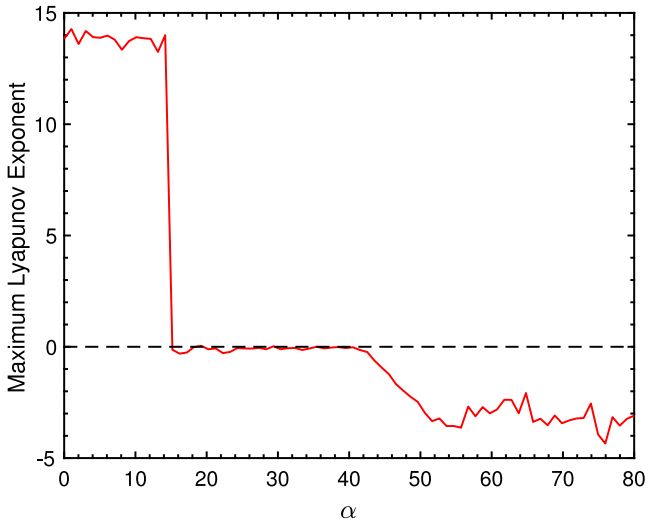

Fig. 7. Maximal Lyapunov exponent for varying α.

growth but is detrimental to the growth of fish. Overall, the fear effect is important in stabilizing the system, and its impact on the densities of phytoplankton and fish is greater than that on the density of zooplankton.

As mentioned previously, α represents the cost of the fear while β denotes the benefit of the fear. The effect of varying α has been already deliberately investigated. By carrying out similar arguments, one can explore the effect of varying β. The approach and the biological scenarios are very similar. So, the details of the discussion are omitted.

4.4. *Effect of fish's food habits*

In the previous discussion, the omnivorous zooplankton is considered. Additionally, in various aquatic ecosystems, different aquatic ecosystems host fish with distinct food habits, which can be broadly categorized as omnivorous, herbivorous, carnivorous, and planktonic [49]. The different food habits of fish may lead to different dynamics of the system. In the following, we examine how these food habits affect the dynamic evolution of the system.

In (2.2), a_3 characterizes the degree of omnivory of the fish. In the following, two different scenarios are investigated: $a_3 = 0$ and

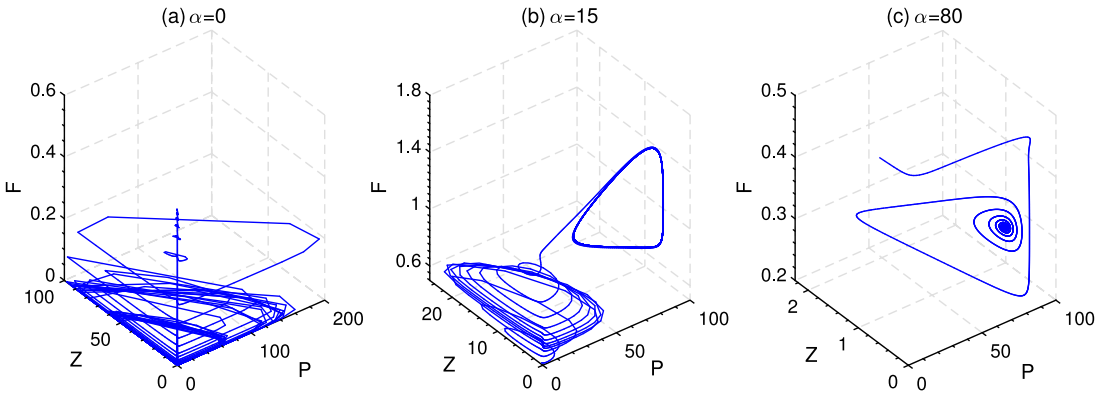

Fig. 8. Attractors of system (2.2) in phase space with different α. (a) $\alpha = 0$, the system admits chaotic dynamics; (b) $\alpha = 15$, the phase trajectories tend to a stable limit circle; (c) $\alpha = 80$, E^* is an attractor. Here $I_0 = 300, N_0 = 10$, other parameter values are listed in Table 1, and $P(0) = 0.7$, $Z(0) = 0.6$, and $F(0) = 0.5$.

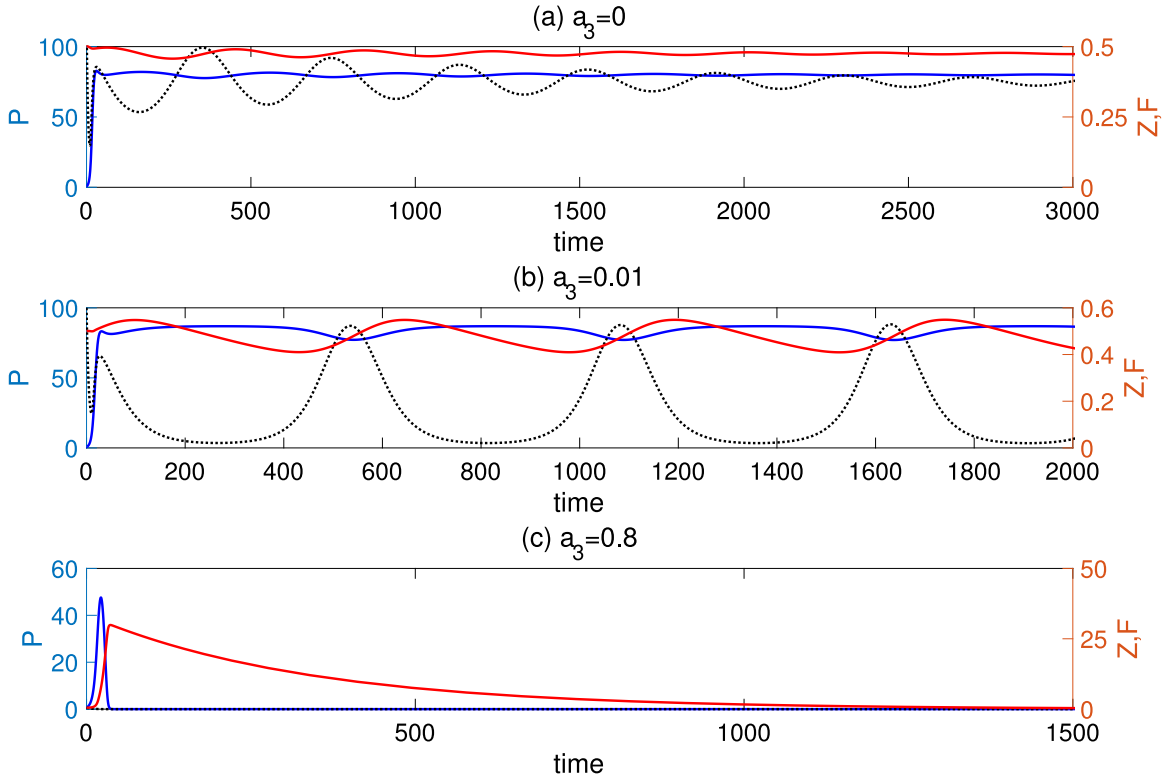

Fig. 9. Time-series of system (2.2) with different a_3 in the presence of the fear effect ($\alpha = 50$). The system exhibits different dynamics: (a) stable coexistence, (b) cyclic coexistence, and (c) extinction of all three populations due to too high predation rate of fish on phytoplankton.

$a_3 \neq 0$. When $a_3 = 0$, the fish only feeds on zooplankton, while, when $a_3 \neq 0$, the fish feeds on both zooplankton and phytoplankton. In the first situation, fish is considered as a planktivorous population and its growth is solely dependent on zooplankton [7]. Fig. 9(a) displays the system's time series in this scenario. Without the predation of fish on phytoplankton, the phytoplankton, zooplankton, and fish can coexist at an interior equilibrium.

The time series with varying attacking rates a_3 of fish on phytoplankton is generated. Fig. 9(b) shows that, when the fish start to attack the phytoplankton (a_3=0.01), (2.2) displays periodic oscillations, a phenomenon known as the enrichment paradox [29,50]. However, when the predation rate a_3 is sufficiently large (a_3=0.8), all three populations tend to extinction (see Fig. 9(c)). It is because of the significant reductions in phytoplankton have made it impossible for zooplankton and fish to survive as well. Therefore, the above analyses suggest that the presence of fish predation on phytoplankton can destabilize the system, and increasing the strength of omnivory can completely destroy it.

In the above, the impact of light (I_0), phosphorus (N_0), fear (α), and fish's food habits (a_3) are well explored numerically by single parameter bifurcation or time series analyses. In order to better understand the combined effect of varying parameters, two-parameter bifurcations can be further explored. For example, Figs. 10 and 11 present the two-parameter bifurcations with I_0-α and N_0-α being the bifurcation parameters, respectively, and the bifurcation surfaces are visualized for phytoplankton, zooplankton, and fish. The numerical simulations show that, when the fear factor α is small, the dynamics of the three populations are more affected by I_0, while when the fear factor α is large, the fear factor has a stabilizing effect on the system, in particular, large fear effects may cause zooplankton to become extinct. In summary, the numerical analyses illustrate that the variation of two parameters has a significant effect on the dynamics of the system.

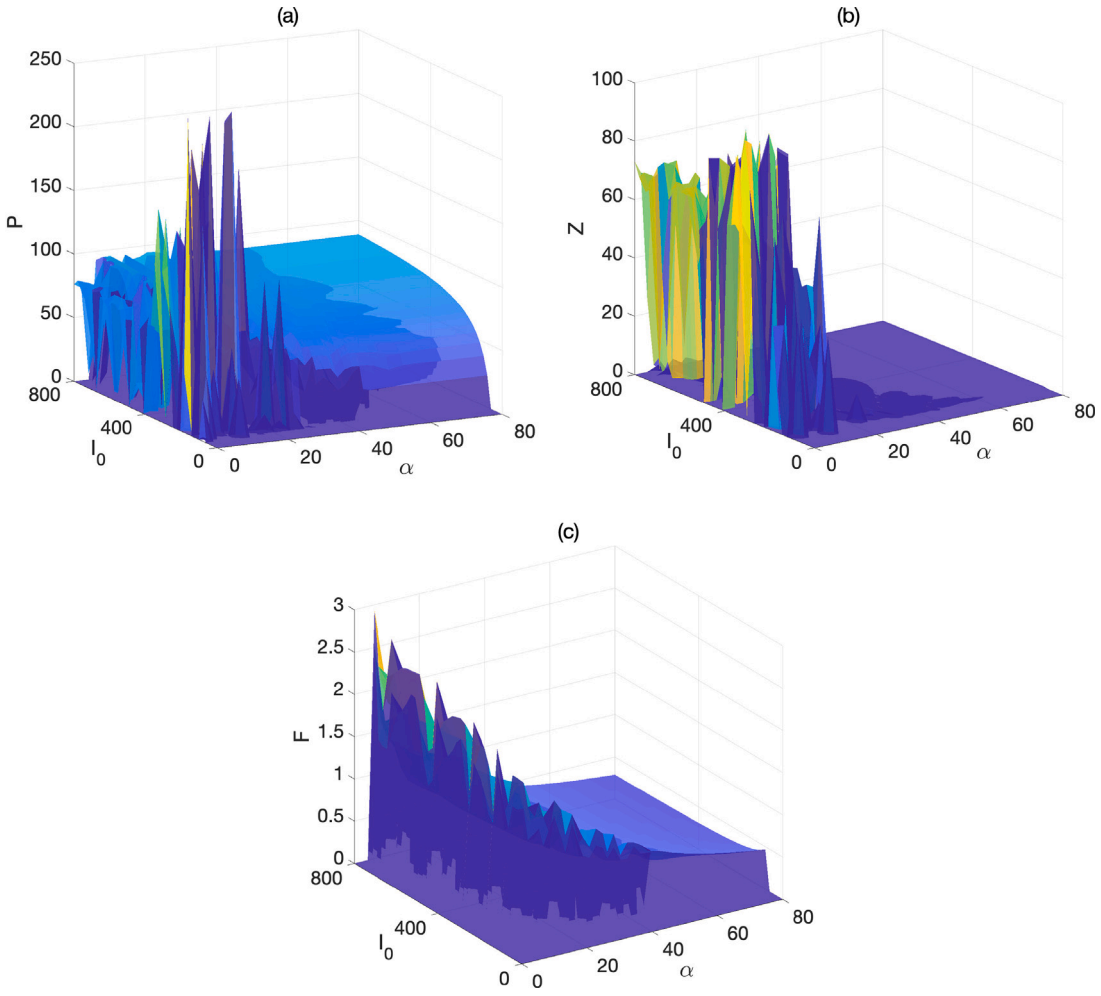

Fig. 10. Bifurcation surfaces for phytoplankton, zooplankton, and fish, respectively, with α and I_0 being the bifurcation parameters. Here $N_0 = 10$, other parameter values are listed in Table 1 except α and I_0.

5. Conclusion and discussion

In aquatic systems, light intensity and phosphorus availability determine the quality of primary producers, which in turn determine the efficiency of nutrient transfer and thereby affect ecosystem functioning. This perspective motivates us to design a tri-trophic level stoichiometry model (2.2) to describe the interactions among phytoplankton, phosphorus cell quota of phytoplankton, dissolved phosphorus, zooplankton, and fish in a well-mixed water column. Different from other stoichiometric models, the fear effect of fish on zooplankton is also explicitly taken into account in this model, thus, the zooplankton ingestion rate depends not only on the producer's quality but also on the fish population.

Theoretical analyses are conducted to investigate the dissipativity of the solution and the existence and stability of equilibria. Analytical results show that there always exists an extinction equilibrium, and if the death rate of phytoplankton is large enough, all three populations eventually tend to extinction, no matter how sensitive the zooplankton is to potential dangers from fish. The low death rate of phytoplankton can guarantee the existence of E_2, in this case, the phytoplankton survive in an aquatic environment. Constraints on d_z (d_f) assure that both phytoplankton and zooplankton (fish) coexist in an aquatic ecosystem.

Numerical simulations are conducted to show the potential roles of the four factors (light, dissolved phosphorus input, fear effect, and fish's food habits) playing in the system dynamics. It can be seen that, when the light intensity is low, the system tends to the extinction equilibrium E_1 since low light intensity is not sufficient to sustain phytoplankton and eventually affects the survival of zooplankton and fish. Moreover, increasing light intensity leads to an obvious shift in the status of three populations, from extinction to coexistence of three populations. Numerical simulations also elaborate that, with increasing I_0, the density of phytoplankton increases and the density of fish decreases, the zooplankton is less sensitive to the variation of light intensity.

The dynamical behavior of system (2.2) is strongly influenced by changes in dissolved phosphorus input concentration. With increasing N_0, the system undergoes a Hopf bifurcation and transitions from a stable equilibrium to periodic oscillations, and the system exhibits a chaotic behavior at higher level of dissolved phosphorus input concentration.

Notably, numerical simulations indicate that the fear effect can transmit the system from chaotic dynamics to periodic oscillations to stable equilibrium via Hopf bifurcation. This finding confirms the role of the fear effect in stabilizing the system. In addition, when the intensity of the fear effect reaches a certain level, the increased level of fear favors the growth of phytoplankton, but not that of fish.

The time series of the system with different a_3 illustrates that fish's food habits play a significant role in the system. Fish grazing on phytoplankton causes the system to shift from convergence to an internal equilibrium to the emergence of cyclic oscillations. Large enough a_3 makes all three populations go extinct. This scenario can be attributed to the increased predation of fish on phytoplankton, which in turn affects the survival of zooplankton and fish.

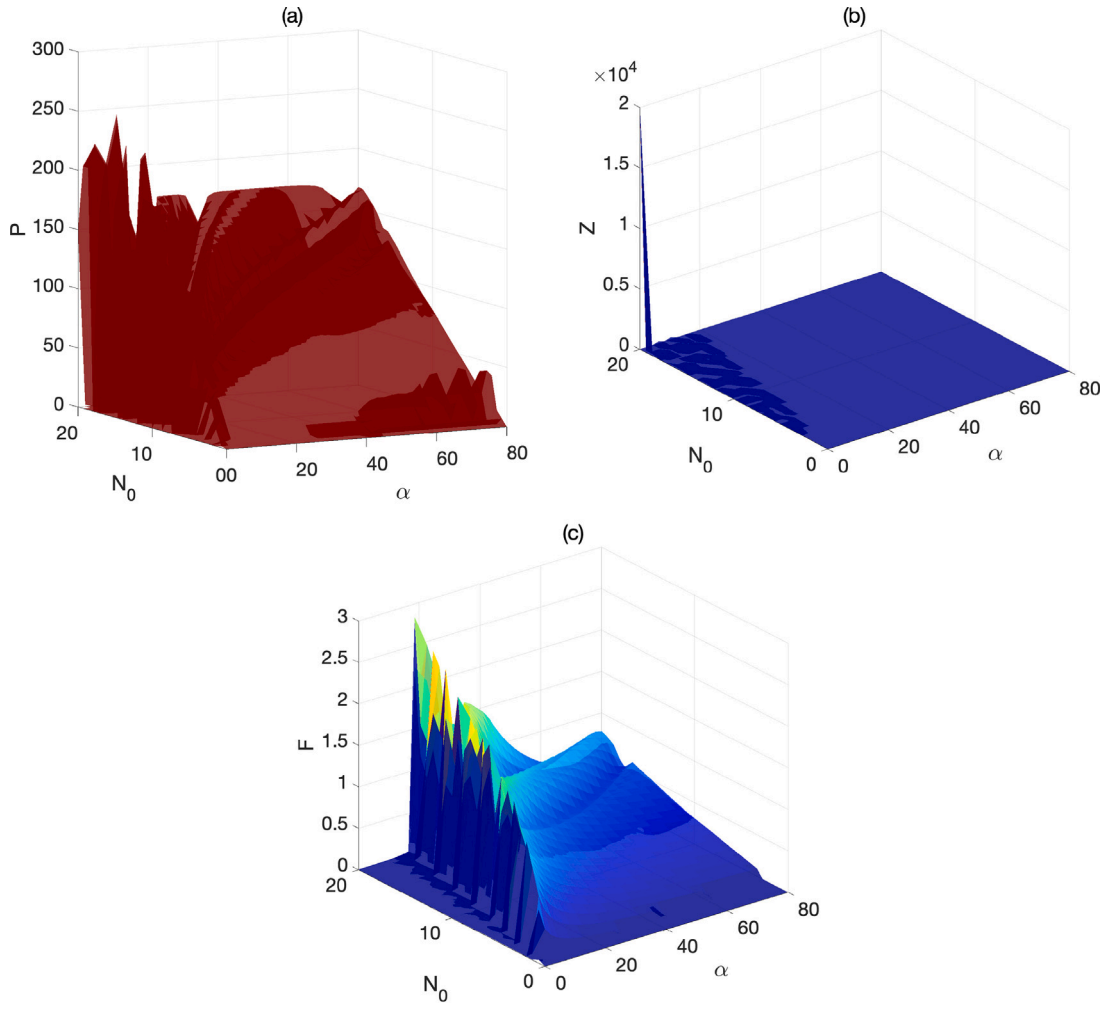

Fig. 11. Bifurcation surfaces for phytoplankton, zooplankton, and fish, respectively, with α and N_0 being the bifurcation parameters. Here $I_0 = 400$, other parameter values are listed in Table 1 except α and N_0.

In summary, the main findings in this study shed some new light on the dynamics of the target system and can be applied to some practical problems in aquatic ecosystems such as controlling algae bloom and increasing the population size of economically significant fish, and so on. In fact, there are many important issues that deserve further exploration. In (2.2), the functional responses of Holling type II are adopted to characterize the predation of fish on zooplankton and phytoplankton, and the fish predation on each of them is assumed to be independent. However, the predation process of fish on phytoplankton and zooplankton occurs simultaneously. So, the predation process of fish should be formulated in a unified way and a more realistic functional response should be incorporated.

In addition, according to the key motivation of the current study, only the stability of the boundary equilibria of model (2.2) are well explored and expounded. More dynamical properties of the model need further rigorous exploration such as the existence and stability of the internal equilibrium, bifurcation analysis, existence and property of strange attractors in chaotic dynamics, and so forth, which call for new approaches and new methods.

CRediT authorship contribution statement

Pingping Cong: Writing – review & editing, Writing – original draft, Validation, Software, Methodology, Formal analysis. **Meng Fan:** Writing – review & editing, Writing – original draft, Validation, Supervision, Methodology, Formal analysis. **Xingfu Zou:** Writing – review & editing, Writing – original draft, Validation, Supervision, Methodology, Formal analysis.

Declaration of competing interest

All authors report there are no conflicts of interest related to the present article.

Data availability

No data was used for the research described in the article.

Acknowledgments

This work was completed when Pingping Cong was visiting the University of Western Ontario (UWO) and she would like to thank the staff of the Department of Mathematics at UWO for their hospitality and help, and thank the UWO for its excellent facilities and support during her visit.

References

[1] J.J. Elser, D.R. Dobberfuhl, N.A. MacKay, et al., Organism size, life history, and N: P stoichiometry: toward a unified view of cellular and ecosystem processes., BioScience 46 (9) (1996) 674–684.

[2] I. Loladze, Y. Kuang, J.J. Elser, Stoichiometry in producer-grazer systems: linking energy flow with element cycling, Bull. Math. Biol. 62 (6) (2000) 1137–1162.
[3] R.W. Sterner, J.J. Elser, Ecological Stoichiometry: The Biology of Elements From Molecules to The Biosphere, Princeton University Press, 2002.
[4] D.O. Hessen, G.I. Agren, T.R. Anderson, et al., Carbon sequestration in ecosystems: the role of stoichiometry, Ecology 85 (5) (2004) 1179–1192.
[5] T.R. Anderson, M. Boersma, D. Raubenheimer, Stoichiometry: linking elements to biochemicals, Ecology 85 (5) (2004) 1193–1202.
[6] Y.H. Du, S.B. Hsu, Concentration phenomena in a nonlocal quasi-linear problem modelling phytoplankton II: Limiting profile, SIAM J. Math. Anal. 40 (4) (2008) 1441–1470.
[7] E.M. Dickman, J.M. Newell, M.J. González, et al., Light, nutrients, and food-chain length constrain planktonic energy transfer efficiency across multiple trophic levels, Proc. Natl. Acad. Sci. 105 (47) (2008) 18408–18412.
[8] H. Wang, H.L. Smith, Y. Kuang, et al., Dynamics of stoichiometric bacteria-algae interactions in the epilimnion, SIAM J. Appl. Math. 68 (2) (2007) 503–522.
[9] A. Peace, Y.Q. Zhao, I. Loladze, et al., A stoichiometric producer-grazer model incorporating the effects of excess food-nutrient content on consumer dynamics, Math. Biosci. 244 (2) (2013) 107–115.
[10] Y. Kuang, J. Huisman, J.J. Elser, Stoichiometric plant-herbivore models and their interpretation, Math. Biosci. Eng. 1 (2) (2004) 215–222.
[11] H. Wang, Y. Kuang, I. Loladze, Dynamics of a mechanistically derived stoichiometric producer-grazer model, J. Biol. Dyn. 2 (3) (2008) 286–296.
[12] X.S. Yang, X. Li, H. Wang, et al., Stability and bifurcation in a stoichiometric producer-grazer model with knife edge, SIAM J. Appl. Dyn. Syst. 15 (4) (2016) 2051–2077.
[13] L.N. Hao, M. Fan, X. Wang, Effects of nutrient enrichment on coevolution of a stoichiometric producer-grazer system, Math. Biosci. Eng. 11 (4) (2014) 841.
[14] M. Chen, M. Fan, Y. Kuang, Global dynamics in a stoichiometric food chain model with two limiting nutrients, Math. Biosci. 289 (2017) 9–19.
[15] J.P. Grover, Stoichiometry, herbivory and competition for nutrients: simple models based on planktonic ecosystems, J. Theoret. Biol. 214 (4) (2002) 599–618.
[16] L.D.J. Kuijper, B.W. Kooi, T.R. Anderson, et al., Stoichiometry and food-chain dynamics, Theor. Popul. Biol. 66 (4) (2004) 323–339.
[17] A. Peace, Effects of light, nutrients, and food chain length on trophic efficiencies in simple stoichiometric aquatic food chain models, Ecol. Model. 312 (2015) 125–135.
[18] C.M. Heggerud, H. Wang, M.A. Lewis, Transient dynamics of a stoichiometric cyanobacteria model via multiple-scale analysis, SIAM J. Appl. Math. 80 (3) (2020) 1223–1246.
[19] T.M. Zaret, J.S. Suffern, Vertical migration in zooplankton as a predator avoidance mechanism, Limnol. Oceanogr. 21 (6) (1976) 804–813.
[20] Z.M. Gliwicz, J. Pijanowska, Effect of predation and resource depth distribution on vertical migration of zooplankton, Bull. Mar. Sci. 43 (3) (1988) 695–709.
[21] Z.M. Gliwicz, Relative significance of direct and indirect effects of predation by planktivorous fish on zooplankton, Hydrobiologia 272 (1) (1994) 201–210.
[22] K.L. Pangle, S.D. Peacor, O.E. Johannsson, Large nonlethal effects of an invasive invertebrate predator on zooplankton population growth rate, Ecology 88 (2) (2007) 402–412.
[23] L.Y. Zanette, A.F. White, M.C. Allen, et al., Perceived predation risk reduces the number of offspring songbirds produce per year, Science 334 (6061) (2011) 1398–1401.
[24] J.P. Suraci, M. Clinchy, L.M. Dill, et al., Fear of large carnivores causes a trophic cascade, Nature Commun. 7 (2016) 10689.
[25] X.Y. Wang, L.Y. Zanette, X.F. Zou, Modelling the fear effect in predator–prey interactions, J. Math. Biol. 73 (5) (2016) 1179–1204.
[26] Y. Wang, X.F. Zou, On mechanisms of trophic cascade caused by anti-predation response in food chain, Math. Appl. Sci. Eng. 1 (2) (2020) 181–206.
[27] R.P. Kaur, A. Sharma, A.K. Sharma, Impact of fear effect on plankton-fish system dynamics incorporating zooplankton refuge, Chaos Solitons Fractals 143 (2021) 110563.
[28] Sajan, S.K. Sasmal, B. Dubey, A phytoplankton-zooplankton-fish model with chaos control: In the presence of fear effect and an additional food, Chaos 32 (1) (2022) 013114.
[29] B. Dubey, S.K. Sasmal, Chaotic dynamics of a plankton-fish system with fear and its carry over effects in the presence of a discrete delay, Chaos Solitons Fractals 160 (2022) 112245.
[30] S. Diehl, S. Berger, R. Wöhrl, Flexible nutrient stoichiometry mediates environmental influences on phytoplankton and its resources, Ecology 86 (11) (2005) 2931–2945.
[31] Y.W. Yan, J.M. Zhang, H. Wang, Dynamics of stoichiometric autotroph-mixotroph-bacteria interactions in the epilimnion, Bull. Math. Biol. 84 (1) (2022) 1–30.
[32] J.M. Medina-Sánchez, M. Villar-Argaiz, P. Carrillo, Neither with nor without you: A complex algal control on bacterioplankton in a high mountain lake, Limnol. Oceanogr. 49 (5) (2004) 1722–1733.
[33] S.A. Berger, S. Diehl, T.J. Kunz, et al., Light supply, plankton biomass, and seston stoichiometry in a gradient of lake mixing depths, Limnol. Oceanogr. 51 (4) (2006) 1898–1905.
[34] H.V. Moeller, M.G. Neubert, M.D. Johnson, Intraguild predation enables coexistence of competing phytoplankton in a well-mixed water column, Ecology 100 (12) (2019) e02874.
[35] K.W. Crane, J.P. Grover, Coexistence of mixotrophs, autotrophs, and heterotrophs in planktonic microbial communities, J. Theoret. Biol. 262 (3) (2010) 517–527.
[36] K. Yoshiyama, H. Nakajima, Catastrophic transition in vertical distributions of phytoplankton: alternative equilibria in a water column, J. Theoret. Biol. 216 (4) (2002) 397–408.
[37] K.F. Edwards, Mixotrophy in nanoflagellates across environmental gradients in the ocean, Proc. Natl. Acad. Sci. 116 (13) (2019) 6211–6220.
[38] T. Andersen, Pelagic Nutrient Cycles: Herbivores as Sources and Sinks, Springer-Verlag, 1997.
[39] J. Urabe, R.W. Sterner, Regulation of herbivore growth by the balance of light and nutrients, Proc. Natl. Acad. Sci. 93 (16) (1996) 8465–8469.
[40] S.E. Jørgensen, S.N. Nielsen, L.A. Jørgensen, Handbook of Ecological Parameters and Ecotoxicology, Elsevier Science Publisher, 1991.
[41] U. Magnea, R. Sciascia, F. Paparella, et al., A model for high-altitude alpine lake ecosystems and the effect of introduced fish, Ecol. Model. 251 (2013) 211–220.
[42] P.P. Cong, M. Fan, X.F. Zou, Dynamics of a three-species food chain model with fear effect, Commun. Nonlinear Sci. Numer. Simul. 99 (2021) 105809.
[43] J. Huisman, F.J. Weissing, Light-limited growth and competition for light in well-mixed aquatic environments: An elementary model, Ecology 75 (2) (1994) 507–520.
[44] R.W. Sterner, D.O. Hessen, Algal nutrient limitation and the nutrition of aquatic herbivores, Annu. Rev. Ecol. Syst. 25 (1994) 1–29.
[45] D.O. Hessen, The algae-grazer interface: feedback mechanisms linked to elemental ratios and nutrient cycling, Arch. Hydrobiol. Beihilfe Ergebnisse Limnol. 35 (1992) 111–120.
[46] R. Motro, I. Ayalon, A. Genin, Near-bottom depletion of zooplankton over coral reefs: III: vertical gradient of predation pressure, Coral Reefs 24 (1) (2005) 95–98.
[47] M. Chen, M. Fan, R. Liu, et al., The dynamics of temperature and light on the growth of phytoplankton, J. Theoret. Biol. 385 (2015) 8–19.
[48] J.M. Zhang, P.P. Cong, M. Fan, Interactions between pelagic and benthic produers: asymmetric competition for light and nutrients, SIAM J. Appl. Math. 83 (2) (2023) 530–552.
[49] X.L. Ma, C.Q. Liu, L.S. Liu, et al., Study on the food web of fish in baiyangdian lake based diet analysis, J. Hydroecol. 32 (4) (2011) 85–90.
[50] M.L. Rosenzweig, Paradox of enrichment: destabilization of exploitation ecosystems in ecological time, Science 171 (3969) (1971) 385–387.